JACS
JOURNAL OF THE AMERICAN CHEMICAL SOCIETY

Article

pubs.acs.org/JACS

Free Fructose Is Conformationally Locked

Emilio J. Cocinero,*[,†] Alberto Lesarri,*[,‡] Patricia Écija,[†] Álvaro Cimas,[§] Benjamin G. Davis,[∥] Francisco J. Basterretxea,[†] José A. Fernández,[†] and Fernando Castaño[†]

[†]Departamento de Química Física, Facultad de Ciencia y Tecnología, Universidad del País Vasco (UPV-EHU), Apartado 644, 48080 Bilbao, Spain

[‡]Departamento de Química Física y Química Inorgánica, Facultad de Ciencias, Universidad de Valladolid, 47011 Valladolid, Spain

[§]Centro de Investigação em Química, Faculdade de Ciências, Universidade do Porto, 4169-007 Porto, Portugal

[∥]Chemistry Department, Oxford University, Chemistry Research Laboratory, 12 Mansfield Road, OX1 3TA Oxford, United Kingdom

Supporting Information

ABSTRACT: Fructose has been examined under isolation conditions using a combination of UV ultrafast laser vaporization and Fourier-transform microwave (FT-MW) spectroscopy. The rotational spectra for the parent, all (six) monosubstituted ^{13}C species, and two single D species reveal unambiguously that the free hexoketose is conformationally locked in a single dominant β-pyranose structure. This six-membered-chair skeleton adopts a $^{2}C_{5}$ configuration (equivalent to $^{1}C_{4}$ in aldoses). The free-molecule structure sharply contrasts with the furanose form observed in biochemically relevant polysaccharides, like sucrose. The structure of free fructose has been determined experimentally using substitution and effective structures. The enhanced stability of the observed conformation is primarily attributed to a cooperative network of five intramolecular O−H···O hydrogen bonds and stabilization of both endo and exo anomeric effects. Breaking a single intramolecular hydrogen bond destabilizes the free molecule by more than 10 kJ mol^{-1}. The structural results are compared to ribose, recently examined with rotational resolution, where six different conformations coexist with similar conformational energies. In addition, several DFT and ab initio methods and basis sets are benchmarked with the experimental data.

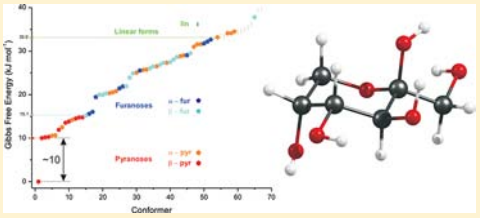

INTRODUCTION

The structural interest in glycobiology has grown in the past decade due to four major chemical issues, conformation, reactivity, solvation, and molecular recognition.[1] The molecular understanding of these problems is essential to describe the biochemical role of sugars, but poses significant challenges even for monosaccharides because of the uncommon combination of tautomeric equilibria, conformational flexibility, large-amplitude intramolecular dynamics, hyperconjugative effects, and anomeric differences.[2] Most of the information on simple sugars has relied on X-ray[3,4] or neutron diffraction[5] studies, which provide atomic resolution for the molecular crystals. However, these data are not transferable to the gas or liquid phases because of the intense crystal packing forces. Moreover, they cannot be directly compared to the diverse theoretical models,[6,7] which are needed for molecular modeling. As a consequence, the description of the intrinsic structural properties and intramolecular dynamics of different sugar families and the validation of theoretical methods are far from assured, requiring detailed experimental information only available through high-resolution spectroscopic methods.

Laser spectroscopy has greatly contributed to the description of sugar conformations and molecular recognition, offering both electronic and vibrational information through UV−UV and IR−UV double-resonance techniques.[8] In particular, laser spectroscopy has been applied to mono-[9,10] and oligosaccharides,[10,11] solvation products,[10,11] and intermolecular complexes.[12] However, both because carbohydrates must be tagged with a chromophore for optical spectroscopy and because vibrational frequencies and electronic transitions are necessarily interpreted with quantum chemical calculations, the structural conclusions are not always unequivocal. Alternatively, pure rotational spectroscopy[13] in the microwave region offers higher (sub-Doppler) frequency resolution, resolving tautomers, isomers, and even isotopologues as totally independent species and thereby providing a more precise route to molecular structures through accurate determination of the moments of inertia. Previous rotational studies of sugars were restricted to small 2- and 3-carbon molecules like glycolaldehyde,[14] glyceraldehyde,[15] or dihydroxyacetone,[16] which could be vaporized via conventional heating. Despite the recent radioastronomical detection of some of these compounds in the interstellar medium presses for more laboratory data, the extension to larger sugar molecules of real biochemical interest was considered impractical because of the thermally labile and/or hygroscopic character of many of these compounds. In this context, we initiated the study of pure carbohydrates in the gas phase with an approach that combines ultrafast UV laser vaporization, jet expansions, and impulse-excitation rotational spectroscopy. This strategy proved successful in the recent investigation of the pentose sugar D-ribose.[2] This analysis of

Received: December 27, 2012
Published: January 24, 2013

   dx.doi.org/10.1021/ja312393m | J. Am. Chem. Soc. 2013, 135, 2845−2852

Scheme 1. Structural Polymorphism in D-Fructose

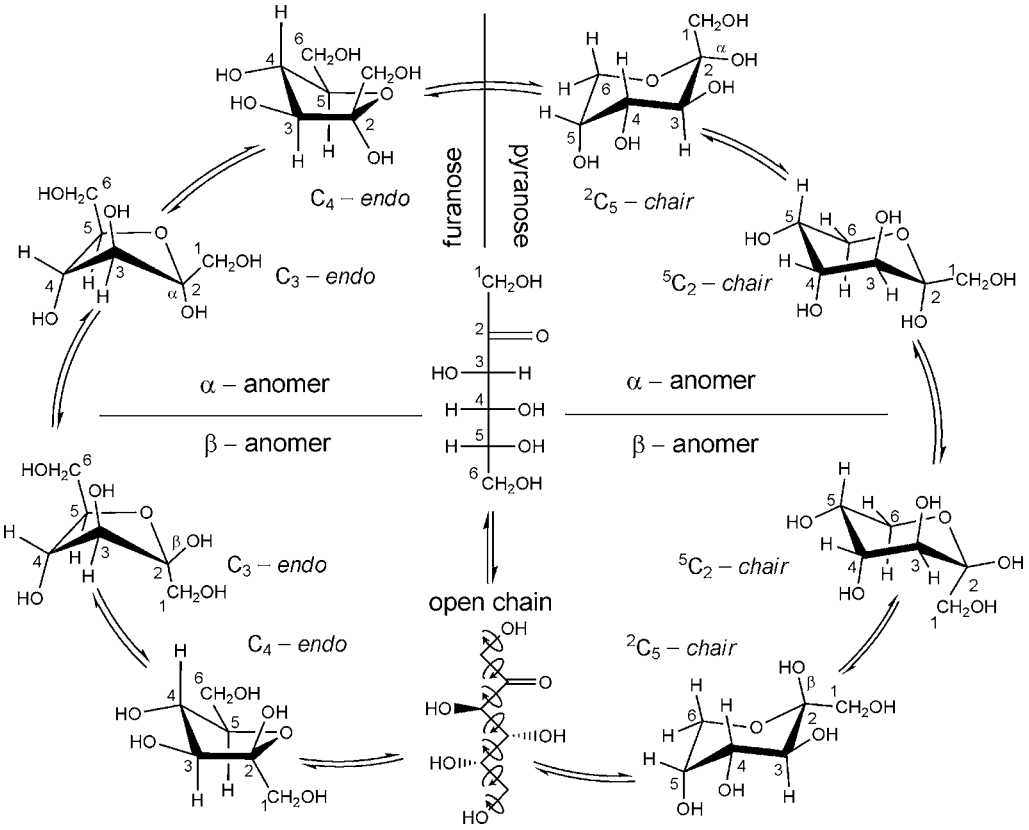

ribose in the gas phase revealed a rich conformational landscape, with the six most stable conformations confined within a small energy window of ca. 4.6 kJ mol^{-1}. Notably, free ribose adopted a tautomeric form not directly relevant to its biological function.

Previous investigations of other chromophore-tagged saccharides show similarly that in most cases several low-lying conformations are populated, but all high-resolution studies to date have been restricted to aldoses, while ketoses remain unexplored. Because the most stable conformations in ribose and other aldoses arise from conflicting contributions from diverse intramolecular effects, it is advisable to extend these structural studies to other free monosaccharides. Here, we report on the conformational and structural properties of the archetypal ketose, D-fructose (Scheme 1). The rotational analysis of this first ketohexose may provide additional clues to understand the delicate balance of intramolecular factors controlling sugar conformation. Our scientific targets for free fructose include determining the tautomeric (pyranose vs furanose or linear chains) and conformational (i.e., $^2C_5$ vs $^5C_2$ in six-membered chairs) preferences, the configuration at the anomeric carbon (α vs β), the conformational distribution, and the role of the intramolecular factors, in particular associative hydrogen bonding. We additionally designed this experiment to observe the most abundant isotopic species of the molecule, thus allowing for the first time a full structural determination of the molecular skeleton of a free sugar. Previous diffraction studies in crystals of fructose are available[4,5] and revealed a $^2C_5$ β-furanose conformation with the exocyclic $-CH_2OH$ group synclinal to the ring oxygen. Conversely, fructose adopts a furanose form in the sucrose disaccharide and glycoysis metabolic pathway. In several solutions, the conformational equilibria favor β-pyranose and β-furanose as dominating species, as observed in ^1H and ^{13}C NMR studies. However, conformational ratios are dependent on the solvents used.[17] There are some previous theoretical studies on fructose, but most of them are now outdated.[6,7] For this reason, our experiment has been supplemented with theoretical calculations intended to test the accuracy of different methods and basis sets. In particular, an extensive conformational search and structural and spectroscopic ab initio and density functional theory (DFT) theoretical predictions were performed.

METHODS

Experimental Section. The rotational spectrum of fructose was measured in a supersonic expansion using a Balle–Flygare[18,19] Fourier-transform microwave (FT-MW) spectrometer built at the UPV-EHU. The spectrometer has been described extensively,[20] so only brief experimental details are provided here. The sample injection system was modified to accommodate a Smalley-type[21] laser ablation source, similar to previous reports.[2,22] D-Fructose ($C_6H_{12}O_6$) was obtained from a commercial supplier (≥99% purity), together with all monosubstituted ^{13}C species ($^{13}CC_5H_{12}O_6$) and the two monodeuterated species at C-1 ($C_6H_{11}DO_6$). The samples were cylindrically pressed with minimum addition of a commercial binder and vaporized with picosecond UV (355 nm) pulses from a Nd:YAG laser (ca. 5 mJ $pulse^{-1}$). The vaporized products are diluted in a flowing current of Ne (6–7 bar), expanding within the chamber of the spectrometer. The jet is probed with short (1 μs) microwave pulses (<10 mW), recording the transient free-induction-decay following molecular polarization. The MW signal detected in the time-domain is later down-converted to the radio frequency region, where it is digitized and Fourier-transformed to the frequency domain. Because of the coaxial arrangement of the jet and the MW radiation, the transition frequencies are split by the Doppler effect, the resonant transitions corresponding to the averaged frequencies. Frequency accuracy is

dx.doi.org/10.1021/ja312393m | J. Am. Chem. Soc. 2013, 135, 2845–2852

better than 3 kHz. Transitions separated less than 10 kHz are resolvable.

Computational. The computational work has been developed in two steps. Initially, an extensive conformational search was accomplished using a fast molecular mechanics method (Merck Molecular Force Field: MMFFs[23]) and advanced Monte Carlo and large-scale low-mode conformational search algorithms. All structures in each structural class (α-/β-pyranose, α-/β-furanose, and linear chains) within an energy window of 20 kJ mol^{-1} were later fully reoptimized using quantum mechanical methods. Following previous experiences to evaluate both the predictive capacity and the computational cost of different computational methods, we compared a pure ab initio method (MP2-full) with two density-functional-theory (DFT) procedures (B3LYP and dispersion-corrected M06-2X[24]). Because of the large number of distinct conformations examined, we used initially a modified cost-effective triple-ζ Dunning's correlation-consistent basis set, denoted minimally augmented, or maug-cc-pVTZ, to calculate the conformational energies.[25] Later, the global minimum was further reinvestigated using the full aug-cc-pVTZ basis set and Pople's 6-311++G(d,p) functions. The vibrational frequency calculations and the rovibronic predictions used the harmonic approximation. In addition, to get a deeper insight into the nature of the stereoelectronic interactions, a Natural Bond Order Analysis (NBO) was performed.[26,27] Finally, zero-point vibrationally averaged structures were calculated using vibrational perturbation theory (VPT2) applied on the B3LYP potential energy surface. In VPT2, the cubic and semidiagonal quartic force constants are computed by finite differentiation of the Hessian along the normal mode coordinates and used to obtain the vibrationally averaged structures at 0 K.[28] Gaussian 09[29] was used in all cases.

RESULTS

Rotational Spectrum. A section of the jet-cooled microwave spectrum of fructose is shown in Figure 1. The spectrum

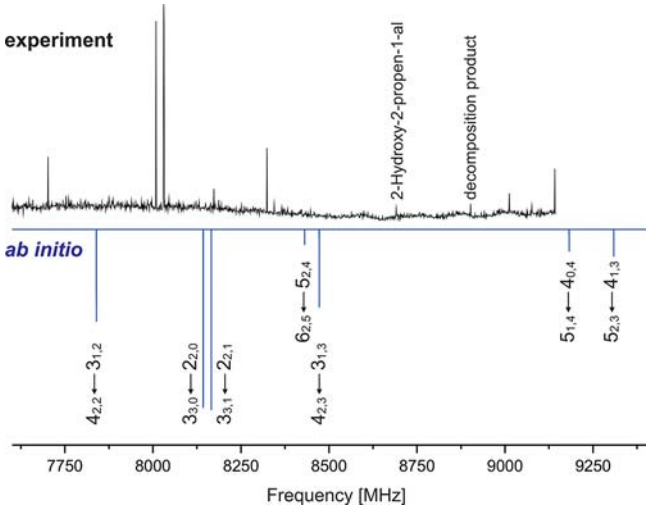

Figure 1. A section of the jet-cooled cm-wave rotational spectrum of fructose (upper trace) and the ab initio simulation (lower trace) at MP2/maug-cc-pVTZ.

was composed of individual transitions with no fine or hyperfine internal structure (as in free ribose), which disappeared when laser vaporization was turned off. The spectrum assignment was guided by the ab initio and DFT conformational searches (Tables S1–S3 in the Supporting Information). However, the theoretical analysis delivered conflicting results, with MP2 and M06-2X suggesting a β-pyranose form (six-membered ring) as global minimum and B3LYP pointing to open chains as predominant forms. We thus focused the first assignment efforts on both plausible structures. Following the initial scans, a series of μ_c R-branch (J+1←J) rotational transitions were eventually assigned. Later, some weaker μ_a rotational transitions were also positively identified. The results of the spectrum fit to the Watson's symetrically reduced semirigid rotor Hamiltonian,[13,30] (I^r representation) are presented in Table 1, and delivered the rotational constants (A, B, C) and some quartic centrifugal distortion parameters (D_J, D_{JK}). A first comparison of the experimental rotational parameters with those predicted theoretically immediately established that the spectrum was generated by a β-pyranose conformation, the linear forms being entirely excluded (large differences of 200–300 MHz in the rotational constants). The rotational predictions for the three theoretical methods are compared to the experiment in Table 1. The spectrum intensities were also consistent with the order-of-magnitude predictions for the electric dipole moment of the predicted β-pyranose (MP2: μ_c = 1.3 D ≫ μ_a = 0.3 D > μ_b = 0.0 D). Following the detection of this first conformer, an exhaustive search for other species was undertaken, but no additional conformations could be detected in the jet-cooled spectrum (some minor decomposition products, i.e., 2-hydroxy-2-propen-1-al, were eventually identified). This fact supports the conclusions from MP2 and M06-2X conformational searches, which suggest that the global minimum of fructose is much more stable (MP2: >10 kJ mol) than other alternative conformations. The MP2 conformational energies are depicted in Figure 2. Finally, the spectral measurements were extended to eight different isotopologues of the observed conformer, comprising all monosubstituted ^{13}C isotopic species and two monodeuterated derivatives at C-1, selected because their position critically depends on the orientation of the exocyclic hydroxy group. The rotational constants of the fructose isotopologues are presented in Table 2 (all observed transitions and residuals are collected as Supporting Information, Tables S4–S12).

Structure. The molecular structure of free fructose was derived from the 27 rotational constants of the detected conformation. Initially, a partial substitution structure was evaluated (r_s), which resulted in the absolute atomic coordinates for the substituted atoms according to the Kraitchmann method.[13,31] A comparison of the experimental coordinates with the ab initio predictions definitively confirmed that the carrier of the spectrum was the predicted β-pyranose global minimum using MP2 and M06-2X theory levels, with differences between experimental and theoretical positions around tens of milliangstroms (Table S13). The resulting structural data are presented in Table 3 and Figure 3, where they are also compared to the near-equilibrium (r_e) theoretical predictions (two coordinates of atom C-2 were constrained to zero because of an accidental near coincidence with the main principal axis). Additionally, an effective structure (r_0) was calculated by a nonlinear least-squares fitting[13,31] of the rotational constants to nine selected structural parameters (mostly ring valence angles and dihedrals). Because of the large number of structural degrees of freedom, the bond lengths and the rest of the molecule were frozen in this case to the MP2 structure (Table S14). The effective and substitution structural data are also compared in Table 3.

DISCUSSION

A single dominant conformation is observed for free fructose in the gas phase. The conformational assignment is unequivocal

Table 1. Rotational Parameters of Fructose and Comparison with Theoretical Predictions

	experiment	MP2/B3LYP/M06-2X aug-cc-pVTZ	MP2/B3LYP/M06-2X maug-cc-pVTZ	MP2/B3LYP/M06-2X 6-311++G(d,p)	B3LYP/maug-cc-pVTZ ground state (v = 0)
A (MHz)[a]	1465.27759(20)[c]	1476.8/1475.7/1460.0	1489.5/1459.5/1475.0	1469.0/1456.5/1473.1	1442.9
B (MHz)	770.56953(11)	777.1/779.1/761.6	785.4/761.7/779.0	777.0/761.0/778.9	754.1
C (MHz)	609.96934(16)	614.8/616.3/602.7	621.7/602.8/616.3	614.1/601.9/615.8	597.1
D_J (kHz)	0.0147(11)	0.017/0.017/0.018	0.018/0.018/0.017	0.017/0.018/0.016	
D_{JK} (kHz)	0.0550(34)	0.037/0.034/0.037	0.038/0.037/0.034	0.035/0.037/0.033	
D_K (kHz)		0.046/0.047/0.054	0.045/0.054/0.046	0.044/0.053/0.042	
d_1 (Hz)		−3.1/−2.9/−3.3	−3.2/−3.3/−2.9	−2.9/−3.2/−2.8	
d_2 (Hz)		−0.60/−0.54/−0.63	−0.60/−0.62/−0.53	−0.55/−0.61/−0.52	
$\lvert\mu_a\rvert$ (D)		0.3/0.3/0.4	0.3/0.4/0.2	0.2/0.3/0.2	
$\lvert\mu_b\rvert$ (D)		0.0/0.0/0.0	0.0/0.0/0.0	0.1/0.0/0.1	
$\lvert\mu_c\rvert$ (D)		1.3/1.3/1.2	1.3/1.2/1.3	1.4/1.3/1.4	
N[b]	37				
σ (kHz)	2.4				

[a]Rotational constants (A, B, C); Watson's quartic centrifugal distortion constants in the S reduction (D_J, D_K, D_{JK}, d_1, d_2); electric dipole moment components (μ_α, $\alpha = a, b, c$, 1 D ≈ 3.336 × 10^{-30} C m) referred to the principal inertial axes. [b]Number of transitions (N) and rms deviation (σ) of the fit. [c]Standard error in parentheses in units of the last digit.

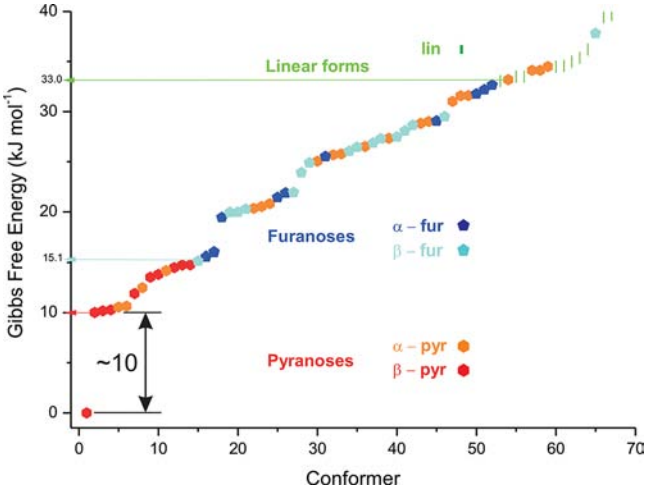

Figure 2. Conformational distribution in free fructose (MP2/maug-cc-pVTZ, see also Table S1).

Table 2. Rotational Parameters of the Monosubstituted Isotopologues of Fructose

	^{13}C-1	^{13}C-2	^{13}C-3
A (MHz)[a]	1461.73953(23)[c]	1465.32149(15)	1461.35512(20)
B (MHz)	764.21762(16)	769.50555(11)	770.37943(15)
C (MHz)	606.47413(29)	609.30381(29)	609.36077(43)
N[b]	19	18	17
σ (kHz)	3.4	1.8	2.4
	^{13}C-4	^{13}C-5	^{13}C-6
A (MHz)[a]	1463.46869(18)	1460.57013(14)	1450.30093(12)
B (MHz)	767.82996(12)	767.00382(12)	769.81132(10)
C (MHz)	608.23613(22)	607.07418(18)	607.56728(16)
N	19	18	18
σ (kHz)	2.7	2.1	1.9
	D_R-C-2		D_S-C-2
A (MHz)[a]	1450.48648(10)		1454.38625(15)
B (MHz)	762.129210(91)		762.80204(13)
C (MHz)	607.20933(45)		604.41366(81)
N	9		8
σ (kHz)	0.9		1.2

[a]Rotational constants (A, B, C). [b]Number of transitions (N) and rms deviation (σ) of the fit. [c]Standard error in parentheses in units of the last digit.

from the detection of multiple isotopic species, which resulted in the atomic substitution coordinates for the carbon skeleton and two hydrogen atoms. An alternative effective structure calculation consistently reproduced the same conformation. According to the structural data, the six-carbon ketose adopts preferentially a β-pyranose $^2C_5$-chair configuration (essentially equivalent to the $^1C_4$ chair of aldoses), with the exocyclic $-CH_2-OH$ hydroxymethyl group equatorial at the anomeric carbon. Characteristically, all of the hydroxy groups are linked together by a cooperative network of intramolecular O−H···O hydrogen bonds. As observed in Figure 4, even the exocyclic hydroxymethyl substituent, which could adopt a free orientation, interacts with the endocyclic O atom (gauche to O6: G+) to behave both as a hydrogen-bond acceptor from O2−H and as a hydrogen-bond donor to the endocyclic O6 oxygen, finally forming a sequence of five correlative hydrogen bonds O5−H→O4−H→O3−H→O2−H→O1−H→O6. This network is quite unique in the context of free glycans as result of the additional exocyclic hydroxymethyl. The hydrogen-bond distances are conditioned in this configuration by the equatorial (Eq) or axial (Ax) configuration of adjacent hydroxy groups, following a sequence Ax (O5)−Eq (O4)−Eq (O3)−Ax (O2) with distances ranging from r_{Ax-Eq} = 2.23−2.25 Å to r_{Eq-Eq} = 2.37 Å. Employing a conventional notation based on Figure 4 and two (±gauche/trans) dihedrals for O1−C1−C2−O6 and H−O1−C1−C2, the observed conformation is oriented counter-clockwise (cc, viewed from above), so fructose would be denoted cc-β-Pyr-$^2C_5$-G+G−. Intramolecular hydrogen-bond networks were previously observed in ribose[2] and in other saccharides analyzed vibrationally.[9,10] The number and strength of the intramolecular O−H···O hydrogen bonds are thus the most probable primary factor stabilizing D-fructopyranose, as confirmed by the theoretical conformational search. While the next three most stable conformers are all β-$^2C_5$-pyranosides (Figure S1), there are large energetic penalties for these alternative structures, in sharp contrast with the observed aldoses where several structures exist simultaneously. In particular, ribose showed a distribution of both β- and α-pyranose structures, with a slight preference (≤1 kJ mol^{-1}) for

dx.doi.org/10.1021/ja312393m | J. Am. Chem. Soc. 2013, 135, 2845−2852

Table 3. Structure of Fructose cc-β-Pyr $^2C_5$[a]

	gas phase			
	r_s	r_0	r_e	crystal
$r(C_1-C_2)$	1.521(19)		1.512	1.526
$r(C_2-C_3)$	1.488(27)		1.515	1.542
$r(C_3-C_4)$	1.577(13)		1.512	1.523
$r(C_4-C_5)$	1.510(6)		1.510	1.529
$r(C_5-C_6)$	1.538(6)		1.507	1.511
$r(C_6-O_6)$			1.422	1.430
$r(C_1-D_S)$	1.081(7)		1.082	1.092
$r(C_1-D_R)$	1.101(10)		1.087	1.092
$r(O_1-C_1)$			1.418	1.414
$r(O_2-C_2)$			1.408	1.407
$r(O_3-C_3)$			1.418	1.420
$r(O_4-C_4)$			1.417	1.418
$r(O_5-C_5)$			1.412	1.426
$\angle(C_1-C_2-C_3)$	111(2)	115.2(5)	113.2	111.7
$\angle(C_2-C_3-C_4)$	109.6(13)	111.6(6)	110.1	111.0
$\angle(C_3-C_4-C_5)$	110.7(5)	112.6(2)	110.4	109.2
$\angle(C_4-C_5-C_6)$	108.6(4)	107.3(3)	109.1	110.2
$\angle(C_5-C_6-O_6)$		115.4(7)	112.2	110.9
$\angle(C_2-C_1-D_S)$	112.5(13)		109.7	110.9
$\angle(C_2-C_1-D_R)$	106.8(15)		109.1	108.2
$\angle(C_2-C_1-O_1)$		110.4(4)	109.3	110.9
$\angle(C_3-C_2-O_2)$			106.5	107.6
$\angle(C_4-C_3-O_3)$			110.3	108.8
$\angle(C_5-C_4-O_4)$			107.6	109.1
$\angle(C_6-C_5-O_5)$			108.8	107.5
$\tau(C_1-C_2-C_3-C_4)$	−174.0(17)	−169.6(7)	−172.8	−169.5
$\tau(C_2-C_3-C_4-C_5)$	50(2)	54.2(10)	55.1	53.2
$\tau(C_3-C_4-C_5-C_6)$	−52.0(9)	−55.8(8)	−54.2	−55.0
$\tau(C_4-C_5-C_6-O_6)$			54.8	56.8
$\tau(C_3-C_2-C_1-D_S)$	130.3(10)		−54.4	−178.7
$\tau(C_3-C_2-C_1-D_R)$	−108.2(18)		65.8	−60.7
$\tau(C_3-C_2-C_1-O_1)$			−171.5	58.4
$\tau(C_4-C_3-C_2-O_2)$			66.3	68.3
$\tau(C_5-C_4-C_3-O_3)$			178.9	175.3
$\tau(C_6-C_5-C_4-O_4)$			−174.9	−175.7
$\tau(O_6-C_6-C_5-O_5)$			−66.0	−64.1

[a]Distances and angles in angstroms and degrees, respectively.

the β forms. Additionally, $^1C_4$ and $^4C_1$ pyranose chairs were encountered for the two anomers, although the furanose (a much more common form in biology) and linear chains were not detected because of their higher conformational energies ($\geq$9.1 kJ mol^{-1}). Conversely, the second most stable MP2 conformation in fructose (cc-β-Pyr-$^2C_5$-G+T), almost identical to the global minimum except for the position of a single hydrogen atom breaking the apparently weak hydrogen bond O1−H···O6 ($r_{H\cdots O6}$ = 2.43 Å), is dramatically destabilizing the structure by ca. 10 kJ mol^{-1}.

Because of the conformational preference around the most stable (cc-β-Pyr-$^2C_5$-G+G−) fructose structure, the observation

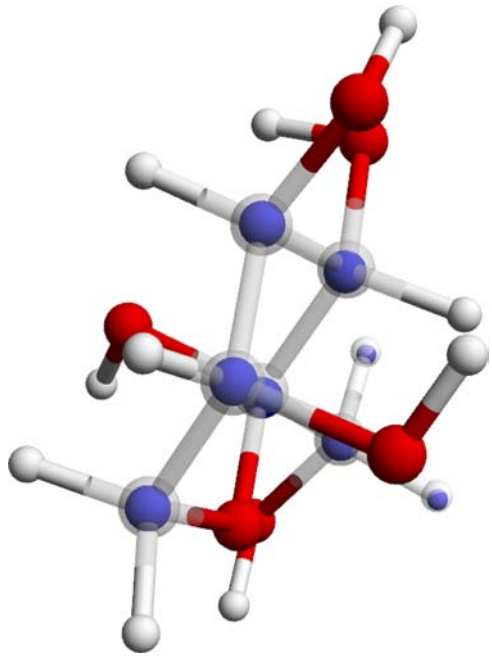

Figure 3. A comparison of the substitution (Tables 3 and S13) and ab initio (Table S14) structures of fructose. The full molecular structure is the theoretical structure. The smaller dark blue spheres are the experimental atom positions for the carbon framework and two substituted hydrogens (note: click model to activate 3D view).

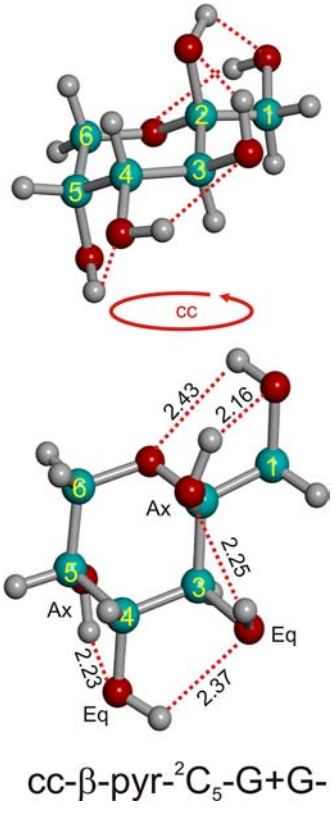

Figure 4. The most stable β-Pyr-$^2C_5$ conformation of fructose is stabilized by a network of five O−H···O intramolecular hydrogen bonds (MP2/maug-cc-pVTZ distances are shown in Table S14). The G+G− orientation of the exocyclic CH_2−OH group is defined by the O1−C1−C2−O6 and H1−O1−C1−C2 dihedrals.

dx.doi.org/10.1021/ja312393m | J. Am. Chem. Soc. 2013, 135, 2845−2852

of a single conformation in the jet is justified. According to the (MP2) theoretical calculations, the population of the observed structure should account for 87.9% of the total population of free fructose at room temperature, and the second lowest-lying energy conformer represents only 1.6% of the total population. The predicted population ratios β-pyr:α-pyr:α-fur:β-fur:linear = 95.9:3.4:0.4:0.3:0.0 show a marked preference for the β-pyranoside form, in contrast with the observations in ribose where β-pyr:α-pyr = 65.4:32.5. We did not consider specifically the possibility of conformational relaxation in the jet to lower-energy structures separated by low barriers (<5−10 kJ mol^{-1}).[32] However, this kind of kinetic process could be predictable for some conformers, as in the two most stable c-α-Pyr-$^5C_2$ conformations differing only in the position of a single hydrogen atom. The higher stability of the cc-β-Pyr-$^2C_5$ configuration is apparent also in the crystal structure, which maintains the same $^2C_5$ conformation. However, the crystal structure differs in the orientation of the exocyclic hydroxymethyl side-chain (G−G+) and the ring hydroxy groups, most likely as a result of the strong crystal packing forces. Notably, the hydrogen-bonding network could not be detected in the solid state, which outlines the importance of the gas-phase studies for this central sugar. Solution studies depend on solvent and experimental conditions, but there is a temperature-dependent preference for the β-pyranose and β-furanose conformations in D_2O, α-pyranose being barely detectable (β-pyr:β-fur:α-fur:α-pyr ≈ 53:32:10:2).[17] In the aprotic solvent d_6-DMSO, the β-pyranose form is present in smaller ratio (β-pyr:β-fur:α-fur:α-pyr ≈ 1:2:1:0), an effect previously attributed to increased intramolecular hydrogen bonding.[33] Notably our work here removes previous ambiguities from solvent work that posed a query about the presence of intramolecular hydrogen bonding. The sharp disagreement between the clear bias seen in the present work (which reveals free fructose in the gas phase for the first time) and that from prior solution studies suggests that solvent effects are more multifaceted than previously realized. The likelihood is that dipole effects perturb the equilibria in DMSO, which are of course absent in our work. We cannot discard the possibility that kinetic effects may restrict the freedom of the mutarotation equilibrium that leads to interconversion of the fructose tautomers, and so our results may simply reflect the tautomer found in its original form prior to entering the gas phase. In the absence of catalyst, this mutarotation is known to be slow, and so gas-phase first-order mutarotation may indeed be absent even under the conditions used here.

Some comparisons with previously available information on molecular conformation of aldoses are tempting. All aldoses analyzed vibrationally are hexoses (glucose, galactose, mannose) or pentoses (xylose) and exhibited several populated conformations, but locked around the $^4C_1$ pyranose chair. Conversely, in the D-ribose pentose, both $^1C_4$ and $^4C_1$ conformations were observed. Finally, fructose has a well-defined $^2C_5$ preferred conformation (equivalent to $^1C_4$ in aldoses). These differences are obviously correlated with the number and type of substituents in the six-membered ring. The phenyl hexopyranosides, like phenyl-D-glucopyranoside, share a common hydroxymethyl substituent at C-5, which is absent in xylose, ribose, or fructose. Furthermore, these phenyl-sugars have a locked anomeric carbon (C-1). On the other hand, fructose displays a hydroxymethyl group in C-1 associated with the ketose form. As a consequence, the larger conformational flexibility of ribose could be connected to the lack of an exocyclic hydroxymethyl substituent. Unfortunately, the monosaccharides for which accurate gas-phase structural information is available are still scarce, so a general comparison of the conformational trends does not seem possible at this time.

The experimental rotational parameters provided an effective benchmark to validate the structural predictions of the ab initio and DFT methods, which might be useful for future studies of monosaccharides. In terms of the conformational search (Tables S1−S3), the B3LYP method systematically favored the acyclic forms, as in ribose,[2] and failed to detect the global minimum. The six most stable B3LYP conformers are open chains, while the experimentally found structure is predicted at 2.8 kJ mol^{-1}. Conversely, MP2 and M06-2X predict that the most stable linear forms are, respectively, 33 and 28 kJ mol^{-1} above their energy origins. This issue most probably hampers the use of the B3LYP method for similar compounds. MP2 and M06-2X give relatively consistent results, with the first eight conformers (β-Pyr and α-Pyr) similarly distributed. Also, the first (β) furanose is predicted at close conformational energies. The comparison of different basis sets in Table 1 gives additionally some hints on the different accuracy of the Dunning's and Pople's triple-ζ basis sets. Most significantly, the reduction of computational cost in maug-cc-pVTZ basis set is barely useful, at least with MP2, because structural accuracy is below the faster Pople function. The larger aug-cc-pVTZ basis set gives improved results, but accuracy is still slightly worse than with the Pople function. Moreover, aug-cc-pVTZ is totally impractical at this time for the conformational search because of the much larger computational cost. In conclusion, the combination of the MP2 method and the Pople basis set represents an effective compromise for our spectroscopic predictions. The M06-2X method, despite empirically accounting for dispersion, turns out to be not as precise as MP2, although it could be a good alternative attending accurate and computational cost. In addition, a large computational effort was performed to predict the rotational constants in the ground state (v = 0) using B3LYP/maug-cc-pVTZ, but surprisingly, it produced worse results than predicting the equilibrium (r_e) rotational constants in Table 1.

The importance and magnitude of steric and hyperconjugative effects on ribose and previously studied aldoses have been barely studied. A natural bond orbital (NBO) analysis revealed the stabilization of the observed structure by *endo*- and *exo*-anomeric effects associated, respectively, with n(O6)→σ*(C2−O2) and n(O2)→σ*(C2−O6) steric and hyperconjugative interactions, and the dominance of *exo*- over the *endo*-anomeric effect, a behavior previously observed using a peptidic model.[13] The dihedral angle O6−C2−O2−H2 of 79.8° is far from the ideal angle of ∼60° (i.e., 64° in ribose) to maximize the *exo*-anomeric effect. This "anomalous behavior" is due to the possibility of extending the network of cooperative hydrogen bonds with an additional interaction O2−H→O1. Moreover, the dihedral angle C2−O2−H2−O1 is 12.2 versus 0° for an ideal hydrogen bond. In consequence, the position of H1 in the observed structure adopts a compromise solution that favors both stabilizations, the interaction O2−H→O1 and the *exo*-anomeric effect.

In summary, the observation of a single structure of fructose in the gas phase can be explained taking into account the juxtaposition of several effects, the presence of a six-membered ring, the extra strength produced by the five consecutive hydrogen bonds, the occurrence of two anomeric effects, and the $^2C_5$-chair configuration. Altogether, these factors favor the

occurrence of the observed conformer over the rest of the explored structures.

The $^2C_5$ pyranose conformation seen here exclusively is a striking outcome not in terms of energetic predictions but from the perspective of the utilization of this structure in biology. It is rare to find this tautomer, and the most widespread form of fructose in nature is the furanose or furanoside (as in sucrose) form. Given the clear bias toward the $^2C_5$ pyranose tautomer that we have observed here, it highlights the dramatic effects that solvent (water) has upon its utilization. Even when found as a ligand in protein systems, the $^2C_5$ pyranose form is rare. Only four structures exist in the Protein Databank in which this free form is preferentially sequestered in this tautomer. In three of those, this form of fructose is merely mimicking other carbohydrate ligands (such as D-mannose[34] or L-fucose[35]). In only one structure [PDB 2FA1] is there a potential speculative role as a functional ligand found bound to the C-terminal domain[36] of a member of the GntR family of transcription factors that have varied roles in metabolism. Notably in this structure a highly solvated fructose ligand is held in the $^2C_5$ fructopyranose form by a bifurcated hydrogen from Arg231 to O6 and OH5 and from the Glu200 to the OH1. In this structure, four additional water molecules hydrogen bond to OH-2,3,4,5, forming an effectively full bridged network. The next result of this overall interaction with solvent and protein is that all of the intramolecular hydrogen bonding that we have observed here for the first time in the naked form of fructopyranose is lost. Together these data suggest that one possible reason for the apparently curious absence of fructopyranose from biology is a propensity to satisfy hydrogen bonding in an intermolecular manner presumably through solvation that overwhelms the inherent energetic biases that we have delineated here. The resultant entropic costs may therefore drive fructose into furanose and furanoside tautomers that may be satisfied with fewer partners. A hunger for solvation may also preclude its ready use as a ligand and would likely lead to effective acid−base interactions for the catalysis of pyranose-to-furanose interconversion. All of these factors may explain the absence of fructofuranose in the gas phase.

■ ASSOCIATED CONTENT

Supporting Information

Tables containing the ab initio (S1) and DFT (S2, S3) conformational searches, the observed list of rotational transitions (S4−S12), atomic substitution coordinates (S13), and ab initio structure of the global minimum (S14), together with a figure (S1) of some of the fructose conformers. This material is available free of charge via the Internet at http://pubs.acs.org.

■ AUTHOR INFORMATION

Corresponding Author

emiliojose.cocinero@ehu.es; lesarri@qf.uva.es

Notes

The authors declare no competing financial interest.

■ ACKNOWLEDGMENTS

Financial support from the Spanish Ministry of Science and Innovation (MICINN, 2010/CSD2007-00013, CTQ2009-14364, CTQ2011-22923), the Basque Government (Consolidated Groups, IT520-10), and UPV/EHU (UFI11/23) is gratefully acknowledged. E.J.C. acknowledges also a "Ramón y Cajal" contract from the MICINN. Computational resources and laser facilities of the UPV-EHU were used in this work (SGIker and I2Basque). A.C. would like to thank Fundação para a Ciência e a Technologia (Lisbon, Portugal) for his "Ciência 2008" contract.

■ REFERENCES

(1) Colins, P.; Ferrier, R. *Monosaccharides: Their Chemistry and Their Roles in Natural Products*; Wiley: New York, 1995.

(2) Cocinero, E. J.; Lesarri, A.; Écija, P.; Basterretxea, F. J.; Grabow, J.-U.; Fernández, J. A.; Castaño, F. *Angew. Chem., Int. Ed.* **2012**, *51*, 3119.

(3) Sisak, D.; McCusker, L. B.; Zandomeneghi, G.; Meier, B. H.; Bläser, D.; Boese, R.; Schweizer, W. B.; Gylmour, R.; Dunitz, J. D. *Angew. Chem., Int. Ed.* **2010**, *49*, 4503.

(4) Kanters, J. A.; Roelofsen, G.; Alblas, B. P.; Meinders, I. *Acta Crystallogr.* **1977**, *B33*, 665.

(5) Takagi, S.; Jeffrey, G. A. *Acta Crystallogr.* **1977**, *B33*, 3510.

(6) (a) Van Eijck, B. P.; Kroon-Batenburg, L. M. J.; Kroon, J. *J. Mol. Struct.* **1990**, *237*, 315. (b) Roberts, C. J.; Debenedetti, P. G. *J. Phys. Chem. B* **1999**, *103*, 7308.

(7) (a) Szarek, W. A.; Korppi-Tommola, S.-L.; Martin, O. R.; Smith, V. H., Jr. *Can. J. Chem.* **1984**, *62*, 1506. (b) Woods, R. J.; Smith, V. H., Jr.; Szarek, W. A. *J. Chem. Soc., Chem. Commun.* **1987**, 937. (c) French, A. D.; Tran, V. *Biopolymers* **1990**, *29*, 1599. (d) Garrett, E. C.; Serianni, A. S. *Carbohydr. Res.* **1990**, *206*, 183. (e) Woods, R. J.; Szarek, W. A.; Smith, V. H., Jr. *J. Am. Chem. Soc.* **1990**, *112*, 4732. (f) Khalil, M.; Woods, R. J.; Weaver, D. F.; Smith, V. H., Jr. *J. Comput. Chem.* **1991**, *12*, 584. (g) French, A. D.; Dowd, M. K.; Reilly, P. J. *J. Mol. Struct. (THEOCHEM)* **1997**, *395−396*, 271. (h) Chung-Phillips, A.; Cheng, Y. Y. *J. Phys. Chem. A* **1999**, *103*, 953. (i) Martins Costa, M. T. C. *Carbohydr. Res.* **2005**, *340*, 2185.

(8) Schermann, J. P. *Spectroscopy and Modelling of Biomolecular Building Blocks*; Elsevier: Amsterdam, 2008.

(9) (a) Talbot, F. O.; Simons, J. P. *Phys. Chem. Chem. Phys.* **2002**, *4*, 3562. (b) Jockusch, R. A.; Talbot, F. O.; Simons, J. P. *Phys. Chem. Chem. Phys.* **2003**, *5*, 1502.

(10) (a) Çarçabal, P.; Jockusch, R. A.; Hünig, I.; Snoek, L. C.; Kroemer, R. T.; Davis, B. G.; Gamblin, D. P.; Compagnon, I.; Oomens, J.; Simons, J. P. *J. Am. Chem. Soc.* **2005**, *127*, 11414. (b) Hünig, I.; Painter, A. J.; Jockusch, R. A.; Çarçabal, P.; Marzluff, E. M.; Snoek, L. C.; Gamblin, D. P.; Davis, B. G.; Simons, J. P. *Phys. Chem. Chem. Phys.* **2005**, *7*, 2474. (c) Çarçabal, P.; Patsias, T.; Hünig, I.; Liu, B.; Kaposta, C.; Snoek, L. C.; Gamblin, D. P.; Davis, B. G.; Simons, J. P. *Phys. Chem. Chem. Phys.* **2006**, *8*, 129. (d) Cocinero, E. J.; Stanca-Kaposta, E. C.; Scanlan, E. M.; Gamblin, D. P; Davis, B. G.; Simons, J. P. *Chem.-Eur. J.* **2008**, *14*, 8947. (e) Cocinero, E. J.; Stanca-Kaposta, E. C.; Dethlefsen, M.; Liu, B.; Gamblin, D. P; Davis, B. G.; Simons, J. P. *Chem.-Eur. J.* **2009**, *15*, 13427.

(11) (a) Jockusch, R. A.; Kroemer, R. T.; Talbot, F. O.; Snoek, L. C.; Çarçabal, P.; Simons, J. P.; Havenith, M.; Bakker, J. M.; Compagnon, I.; Meijer, G.; von Helden, G. *J. Am. Chem Soc.* **2004**, *126*, 5709. (b) Çarçabal, P.; Hünig, I.; Gamblin, D. P.; Liu, B.; Jockusch, R. A.; Kroemer, R. T.; Snoek, L. C.; Fairbanks, A. J.; Davis, B. G.; Simons, J. P. *J. Am. Chem. Soc.* **2006**, *128*, 1976. (c) Stanca-Kaposta, E. C.; Gamblin, D. P.; Cocinero, E. J.; Frey, J.; Kroemer, R. T.; Fairbanks, A. J.; Davis, B. G.; Simons, J. P. *J. Am. Chem. Soc.* **2008**, *130*, 10691. (d) Su, Z.; Wagner, B.; Cocinero, E. J.; Ernst, B.; Simons, J. P. *Chem. Phys. Lett.* **2009**, *477*, 365. (e) Cocinero, E. J.; Gamblin, D. P.; Davis, B. G.; Simons, J. P. *J. Am. Chem. Soc.* **2009**, *131*, 11117.

(12) (a) Screen, J.; Stanca-Kaposta, E. C.; Gamblin, D. P.; Liu, B.; Macleod, N. A.; Snoek, L. C.; Davis, B. G.; Simons, J. P. *Angew. Chem., Int. Ed.* **2007**, *46*, 3644. (b) Stanca-Kaposta, E. C.; Gamblin, D. P.; Screen, J.; Liu, B.; Snoek, L. C.; Davis, B. G.; Simons, J. P. *Phys. Chem. Chem. Phys.* **2007**, *9*, 4444. (c) Su, Z.; Cocinero, E. J.; Stanca-Kaposta, E. C.; Davis, B. G.; Simons, J. P. *Chem. Phys. Lett.* **2009**, *471*, 17. (d) Cocinero, E. J.; Çarçabal, P.; Vaden, T.; Simons, J. P.; Davis, B. G.

Nature **2011**, *469*, 76. (e) Cocinero, E. J.; Çarçabal, P.; Vaden, T.; Davis, B. G.; Simons, J. P. *J. Am. Chem. Soc.* **2011**, *133*, 4548.
(13) Gordy, W.; Cook, R. L. *Microwave Molecular Spectra*; Wiley: New York, 1984.
(14) (a) Butler, R. A. H.; De Lucia, F. C.; Petkie, D. T; Mollendal, H.; Horn, A.; Herbst, E. *Astrophys. J., Suppl. Ser.* **2001**, *134*, 319. (b) Weaver, S. L. W.; Butler, R. A. H.; Drouin, B. J.; Petkie, D. T.; Dyl, K. A.; De Lucia, F. C.; Blake, F. C. *Astrophys. J., Suppl. Ser.* **2005**, *158*, 188. (c) Rey, M.; Aviles-Moreno, J. R.; Huet, T. R. *Chem. Phys. Lett.* **2006**, *430*, 121 and references therein.
(15) Lovas, F. J.; Suenram, R. D.; Plusquellic, D. F.; Mollendal, H. *J. Mol. Spectrosc.* **2003**, *222*, 263.
(16) Weaver, S. L. W.; Braakman, R.; Kent, D. R., IV; Blake, G. A. *J. Mol. Spectrosc.* **2004**, *224*, 101.
(17) (a) Dais, P.; Perlin, A. S. *Carbohydr. Res.* **1985**, *136*, 215. (b) Funcke, W.; von Sonntag, C. *Carbohydr. Res.* **1979**, *75*, 305. (c) Angyal, S. J.; Bethell, G. S. *Aust. J. Chem.* **1976**, *29*, 1249. (d) De Bruyn, A.; Antenius, M.; Verhegge, G. *Carbohydr. Res.* **1975**, *41*, 295. (e) Doddrell, D.; Allerhand, A. *J. Am. Chem. Soc.* **1971**, *93*, 2779. (f) Dais, P. *Carbohydr. Res.* **1987**, *169*, 159.
(18) (a) Balle, T. J.; Flygare, W. H. *Rev. Sci. Instrum.* **1981**, *52*, 33. (b) Grabow, J.-U.; Caminati, W. In *Frontiers of Molecular Spectroscopy*; Laane, J., Ed.; Elsevier: Amsterdam, 2009; Chapter 14.
(19) Grabow, J.-U.; Stahl, W.; Dreizler, H. *Rev. Sci. Instrum.* **1996**, *67*, 4072.
(20) Cocinero, E. J.; Lesarri, A.; Écija, P.; Grabow, J.-U.; Fernández, J. A.; Castaño, F. *Phys. Chem. Chem. Phys.* **2010**, *12*, 12486.
(21) Powers, D. E.; Hansen, S. G.; Geusic, M. E.; Pulu, A. C.; Hopkins, J. B.; Dietz, T. G.; Duncan, M. A.; Langridged-Smith, P. R. R.; Smalley, R. E. *J. Phys. Chem.* **1982**, *86*, 2556.
(22) Alonso, J. L.; Cocinero, E. J.; Lesarri, A.; Sanz, M. E.; López, J. C. *Angew. Chem., Int. Ed.* **2006**, *45*, 3471.
(23) Halgre, T. A. *J. Comput. Chem.* **1999**, *20*, 738.
(24) (a) Zhao, Y.; Truhlar, D. G. *Theor. Chem. Acc.* **2008**, *120*, 215. (b) Zhao, Y.; Truhlar, D. G. *Acc. Chem. Res.* **2008**, *41*, 157.
(25) (a) Papajak, E.; Leverentz, H. R.; Zheng, J.; Thruhlar, D. G. *J. Chem. Theory Comput.* **2009**, *5*, 1197. (b) Papajak, E.; Thruhlar, D. G. *J. Chem. Theory Comput.* **2010**, *6*, 597.
(26) Reed, A. E.; Weinhold, F. *J. Chem. Phys.* **1985**, *78*, 4066.
(27) Foster, J. P.; Weinhold, F. *J. Am. Chem. Soc.* **1980**, *102*, 7211.
(28) Barone, V. *J. Chem. Phys.* **2005**, *122*, 014108.
(29) Frisch, M. J.; et al. *Gaussian 2010*; Gaussian, Inc.: Wallingford, CT, 2010.
(30) Watson, J. K In *Vibrational Spectra and Structure*; Durig, J. R., Ed.; Elsevier: Amsterdam, 1977; Vol. *6*, pp 1− 89.
(31) Rudolph, H. D. In *Advances in Molecular Structure Research*; Hargittai, M., Hargittai, I., Eds.; JAI Press: Greenwich, CT, 1995; Vol. *1*, Chapter 3, pp 63−114.
(32) Ruoff, R. S.; Klots, T. D.; Emilsson, T.; Gutowsky, H. S. *J. Chem. Phys.* **1990**, *93*, 3142.
(33) Jaseja, M.; Perlin, A. S.; Dais, P. *Magn. Reson. Chem.* **1990**, *28*, 283−289.
(34) Doores, K. J.; Fulton, Z.; Hong, V.; Patel, M. K.; Scanlan, C. N.; Wormald, M. R.; Finn, M. G.; Burton, D. R.; Wilson, I. A.; Davis, B. G. *Proc. Natl. Acad. Sci. U.S.A.* **2010**, *107*, 17107−17112.
(35) Loris, R.; Tielker, D.; Jaeger, K. E.; Wyns, L. *J. Mol. Biol.* **2003**, *331*, 861−870.
(36) Gorelik, M.; Lunin, V. V.; Skarina, T.; Savchenko, A. L. *Protein Sci.* **2006**, *15*, 1−15.